

# Convection-Driven Pull-Down Assays in Nanoliter Droplets Using Scaffolded Aptamers

Xiangmeng Qu,<sup>†,‡</sup> Hongbo Zhang,<sup>‡,||</sup> Hong Chen,<sup>\*,§</sup> Ali Aldalbahi,<sup>⊥</sup> Li Li,<sup>†</sup> Yang Tian,<sup>†</sup> David A. Weitz,<sup>‡</sup> and Hao Pei<sup>\*,†</sup>

<sup>†</sup>Shanghai Key Laboratory of Green Chemistry and Chemical Processes, School of Chemistry and Molecular Engineering, East China Normal University, 500 Dongchuan Road, Shanghai 200241, P. R. China

<sup>‡</sup>Harvard John A. Paulson School of Engineering and Applied Sciences, Harvard University, Cambridge, Massachusetts 02138, United States

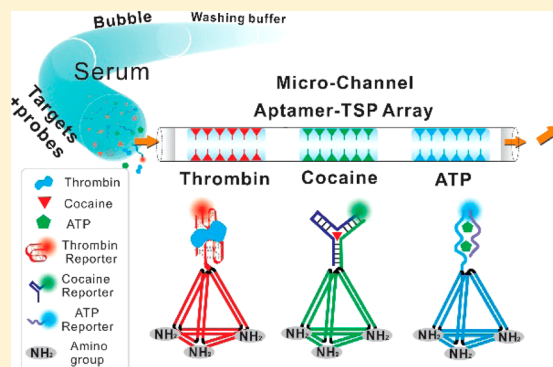
<sup>§</sup>Pen-Tung Sah Institute of Micro-Nano Science and Technology, Xiamen University, Xiamen 361005, P. R. China

<sup>||</sup>Division of Pharmaceutical Chemistry and Technology, Faculty of Pharmacy, University of Helsinki, FI-00014 Helsinki, Finland

<sup>⊥</sup>Chemistry Department, King Saud University, Riyadh 11451, Saudi Arabia

## S Supporting Information

**ABSTRACT:** One of the great challenges in cellular studies is to develop a rapid and biocompatible analytical tool for single-cell analysis. We report a rapid, DNA nanostructure-supported aptamer pull-down (DNAPull) assay under convective flux in a glass capillary for analyzing the contents of droplets with nano- or picoliter volumes. We have demonstrated that the scaffolded aptamer can greatly improve the efficiency of target molecules' pull down. The convective flux allows complete reaction in <5 min, which is an 18-fold improvement compared to purely diffusive flux (traditional model of the stationary case). This established DNAPull assay can serve as a rapid and sensitive analytical platform for analyzing a variety of bioactive molecules, including small molecules [ATP, limit of detection (LOD) of 1  $\mu$ M], a drug (cocaine, LOD of 1  $\mu$ M), and a biomarker (thrombin, LOD of 0.1 nM). Significantly, the designed microfluidic device compartmentalizes live cells into nanoliter-sized droplets to present single-cell samples. As a proof of concept, we demonstrated that cellular molecules (ATP) from a discrete number of HNE1 cells (zero to five cells) lysed inside nanoliter-sized droplets can be analyzed using our DNAPull assay, in which the intracellular ATP level was estimated to be  $\sim$ 3.4 mM. Given the rapid assay feature and single-cell sample analysis ability, we believe that our analytical platform of convection-driven DNAPull in a glass capillary can provide a new paradigm in biosensor design and will be valuable for single-cell analysis.



Single-cell analysis has become a highly promising tool for cellular studies.<sup>1–4</sup> Microfluidic generation of spatially defined droplets with nano- or picoliter volumes is extremely useful in biomedical devices for single-cell samples because their size is comparable to that of living cells and because the samples have high-throughput assay capability.<sup>5–10</sup> Such devices equipped with a rapid and biocompatible analytical tool can provide a powerful and versatile approach for single-cell analysis.<sup>11–15</sup> A simple and direct way is combining a microfluidic platform with a pull-down assay. In the classical pull-down assay, the target molecule (bait) is captured on an immobilized affinity-specific ligand, bringing along its binding partners (prey) from the cell lysate.<sup>16–18</sup> The identity of the prey is usually determined using Western blotting or mass spectrometry. A key advantage of a pull-down assay in microfluidics is that the analyte can be directly visualized from a nano- or picoliter droplet under a fluorescence microscope, bypassing further laborious sample pre-preparation

steps necessary for Western blotting or mass spectrometry. A pull-down assay is similar in methodology to an enzyme-linked immunosorbent assay, both of which are powerful analytical techniques, except that the antigen–antibody interaction is replaced by some other affinity system. It is thus highly desirable to devise an efficient biomolecule-recognition interface for the pull-down assay inside a microfluidic channel.

DNA nanotechnology has attracted intense interest because it allows the functionalization of macroscopic surfaces with atomic spatial precision and versatile functionality,<sup>19–21</sup> thus offering a highly promising approach for the design and construction of an intelligent interface for an efficient pull-down assay. In particular, three-dimensional (3D) DNA tetrahedron architectures, possessing mechanical rigidity and

Received: November 14, 2016

Accepted: February 16, 2017

Published: February 16, 2017



structural stability, have proven to be excellent candidates for immobilizing biomolecules on macroscopic surfaces.<sup>22–28</sup> Taking advantage of the steady structure and consistently favorable orientation of DNA tetrahedron bridges, the capture biomolecules can be directly immobilized on the surface with a specific orientation and well-defined spacing.<sup>28</sup> Many recent advances have demonstrated that DNA tetrahedron-decorated gold surfaces exhibit superior biomolecular recognition and thus hold great promise for the development of high-performance bioassay platforms.<sup>26,28,29</sup> Despite the progress, their practical applications in fluorescence microarrays are still hindered by the complicated fabrication process, together with the high cost and strong fluorescence quenching effect of gold substrates.<sup>30</sup>

Here we developed a rapid DNA nanostructure scaffold-supported aptamer pull-down (DNaPull) assay in a nano- or picoliter droplet, for applications in single-cell analysis. In this design, we employed DNA aptamers to ensure highly selective recognition of target molecules and immobilized them onto the inner surfaces of a glass capillary via a rigid and spatially isolated 3D DNA nanostructure bridge. A bubble-mediated shuttle reaction<sup>31</sup> was introduced to improve the rate of the DNaPull assay by automatic sample delivery and convective transport with pressure-driven fluid flow. An array of DNaPull-based sensors inside a glass capillary can serve as a rapid and highly sensitive multiplex assay to simultaneously detect various bioactive molecules in a nanoliter droplet, including a small molecule (ATP), a biomarker (thrombin), and a drug (cocaine). Importantly, cellular molecules (ATP) can be analyzed using our DNaPull assay by compartmentalizing cells (one to five cells) into nanoliter-sized droplets.

## ■ EXPERIMENTAL SECTION

**Chemicals and Materials.** The glass capillary with a 200  $\mu\text{m}$  inner diameter was purchased from Shanghai Xinpeng Co., Ltd. (Shanghai, P. R. China). The syringe pump (LSP02-1B) was purchased from Baoding Longer Precision Pump Co., Ltd. (Baoding, Hebei, P. R. China). The CCD cameras (TK-C9200EC for capturing videos and a high-performance cooled CCD, Alta U4000, for data collection) were purchased from the JVC (China) Investment Co., Ltd. (Shanghai, P. R. China) and Apogee Instruments Inc. (Roseville, CA), respectively. A green solid state laser (MXL-III-532, 532 nm, 50 mW) was purchased from Changchun New Industries Optoelectronics Technology Co., Ltd. (Changchun, Jilin, P. R. China). A narrow band-pass interference filter (JSL600-25, 600  $\pm$  5 nm, diameter of 25 mm) was purchased from Zolix Instruments Co., Ltd. (Beijing, P. R. China). The luciferin-luciferase-based ATP luminescence assay kit was purchased from Beyotime Biotechnology. Human  $\alpha$ -thrombin, ATP disodium, GTP disodium, and CTP disodium were purchased from HeFei BoMei Biotechnology Co., Ltd. (Hefei, China). UTP trisodium was purchased from Shanghai yuanye Bio-Technology Co., Ltd. (Shanghai, China). ADP disodium, AMP disodium, 3-aminopropyltriethoxysilane (APTES), 25% glutaraldehyde, and tris(hydroxymethyl)-aminomethane were purchased from Sigma-Aldrich; 100 mL of a 10 mM phosphate buffer (PB) (pH 7.4) solution was prepared by mixing 81 mL of a 10 mM  $\text{Na}_2\text{HPO}_4$  aqueous solution with 19 mL of a 10 mM  $\text{NaH}_2\text{PO}_4$  aqueous solution. All oligonucleotides were synthesized and purified by Sangon Biotech Shanghai Co. (Shanghai, China), and DNA sequences and their labeling are listed in Table S1.

**Synthesis of DNA Nanostructure Scaffold-Supported Aptamer Pull-Down (DNaPull) Probes.** The DNaPull probes were formed on the basis of the method reported in ref 30. The four oligonucleotides were mixed stoichiometrically and dissolved in 1 $\times$  TAE/ $\text{Mg}^{2+}$  buffer [40 mM Tris-HCl, 1 mM EDTA, 3 mM  $\text{Na}^+$ , and 12.5 mM  $\text{Mg}^{2+}$  (pH 8.0)] at a final concentration of 10  $\mu\text{M}$ . The mixture was heated to 95  $^\circ\text{C}$  for 2 min and then cooled to 4  $^\circ\text{C}$  within 30 s.

**Sample Assay.** The detection of ATP, cocaine, and thrombin was performed in the sandwich format inside a glass capillary. A bubble-mediated shuttle reaction was introduced, in which the droplets are shuttled back and forth along the glass capillary, which swept over DNaPull probes inside the glass capillary. Specifically, for the ATP assay, four strands, DNaPull-A-ATP, DNaPull-B, DNaPull-C, and DNaPull-D, were annealed to form DNaPull-ATP, which was then used to fabricate microarrays inside the glass capillary. Briefly, 10  $\mu\text{M}$  DNaPull-ATP was dissolved in the immobilization buffer (1.0 M NaCl and 0.15 M  $\text{NaHCO}_3$ ), and the alcohol (butanol, pentanol, or hexanol) acted as the organic carrier fluid. After the probe droplet array was generated along the glass capillary, the glass capillary was then incubated overnight at room temperature to immobilize the probe in the droplets onto the inner wall of the aldehyde-modified glass capillary. After being rinsed with immobilizing buffer and deionized water, the glass capillary was chemically reduced using a  $\text{NaBH}_4$  solution (100 mg of  $\text{NaBH}_4$  dissolved in 30 mL of 1 $\times$  PBS and 10 mL of 95% EtOH) for 45 min, followed by a blocking step using 5% BSA in PBS [20 mM sodium phosphate (pH 7.5), 100 mM NaCl, and 0.1 mM EDTA]. The mixture containing ATP at variable concentrations (1  $\mu\text{M}$ , 10  $\mu\text{M}$ , 100  $\mu\text{M}$ , 250  $\mu\text{M}$ , 500  $\mu\text{M}$ , and 1 mM) and ATP reporter-Cy3 (500 nM) was introduced into the glass capillary, incubated at 37  $^\circ\text{C}$  for 30 min in a humidity chamber, and then washed with washing buffer [twice with PBST (1 $\times$  PBS buffer contains 0.1% Tween 20) buffer and once with PBS buffer]. In a typical experiment, we characterized three replicate assays. For each sample replicate, the fluorescence image of each DNaPull sensor spot after capturing the target molecules was collected by the high-performance cooled CCD camera with an 80 pixel  $\times$  80 pixel region of interest and further analyzed with the MaxIm DL software. The fluorescence intensities were thus averaged over 2400 pixels and three sample replicates with error bars showing the standard deviation. Before use, we randomly selected three from the same batch of DNaPull-ATP assay-functionalized glass capillaries and performed the calibration in the presence of 1000  $\mu\text{M}$  ATP. The system exhibited good reproducibility and batch homogeneity with a standard deviation of <5%. Likewise, for the cocaine assay, DNaPull-A-cocaine (cocaine aptamer), DNaPull-B, DNaPull-C, and DNaPull-D were annealed to form DNaPull-cocaine. DNaPull-cocaine (10  $\mu\text{M}$ ) was then used to fabricate microarrays inside the glass capillary for the cocaine assay. The mixture containing cocaine at variable concentrations (1  $\mu\text{M}$ , 10  $\mu\text{M}$ , 50  $\mu\text{M}$ , 100  $\mu\text{M}$ , 200  $\mu\text{M}$ , 500  $\mu\text{M}$ , and 1 mM) and cocaine reporter-Cy3 (500 nM) was introduced into the glass capillary and incubated at 37  $^\circ\text{C}$  for 30 min in a humidity chamber, followed by the same procedure described for the thrombin assay. The thrombin assay was conducted using a similar procedure except that thrombin at variable concentrations (100 pM, 1 nM, 10 nM, 100 nM, 250 nM, 500 nM, and 1  $\mu\text{M}$ ) was used.

**Multiplex Detection in Serum.** Three types of DNaPull probes (DNaPull-ATP, DNaPull-cocaine, and DNaPull-throm-

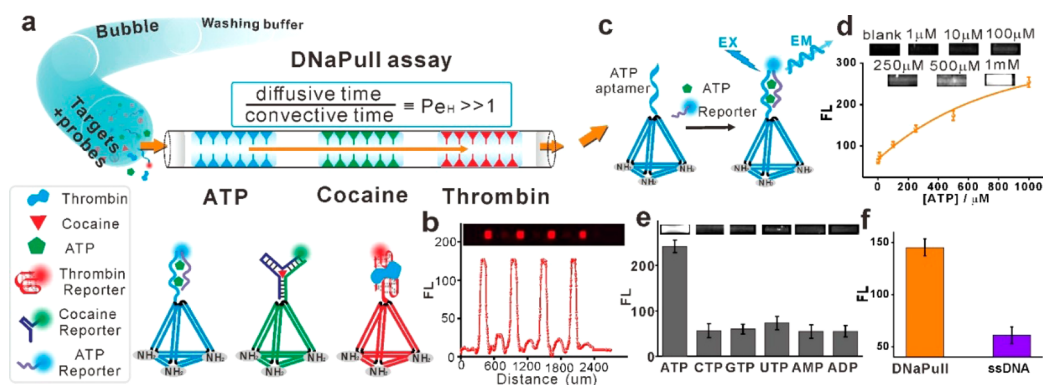


**Figure 1.** (a) Construction of an array of DNaPull-based sensors inside the glass capillary for the detection of ATP, cocaine, and thrombin through a bubble-mediated shuttle reaction process. (b) Spatially defined droplets with a nanoliter in the glass capillary. (c) Construction of a DNaPull-based ATP sensor. (d) Fluorescence intensities and corresponding fluorescent images (inset) of DNaPull probes in the presence of 1, 10, 100, 250, 500, or 1000  $\mu\text{M}$  ATP. (e) Selectivity of the DNaPull-based ATP sensor over CTP, GTP, UTP, ADP, and AMP (all at 1 mM). The corresponding fluorescent images are shown as insets. (f) Comparison of DNaPull- and ssDNA-based sensor performance (with 500  $\mu\text{M}$  ATP).

bin) microarrays were sequentially immobilized along the glass capillaries using a droplet array generator. As schematically illustrated in Figure S2, the slotted vials that contained three types of DNaPull probes (DNaPull-ATP, DNaPull-cocaine, and DNaPull-thrombin), immobilization buffer (1.0 M NaCl and 0.15 M  $\text{NaHCO}_3$ ), and the organic carrier fluid were arranged alternately on a stepping motor. As the stepping motor rotates, the tip of the aldehyde-modified glass capillary sweeps through all the vials. The probe solution flows into the capillary sequentially with the drawing of the syringe pump, and then an array of probe droplets in the carrier is formed along the glass capillary automatically, followed by the same chemical reducing and blocking treatment as described for the preparation of the ATP assay. Subsequently, serum sample 1 (50% serum, blank, row 1), serum sample 2 (250  $\mu\text{M}$  ATP and 500 nM ATP reporter-Cy3 in 50% serum, row 2), serum sample 3 (100  $\mu\text{M}$  cocaine and 500 nM cocaine reporter-Cy3 in 50% serum, row 3), serum sample 4 (100 nM human  $\alpha$ -thrombin and 500 nM thrombin reporter-Cy3 in 50% serum, row 4), serum sample 5 (250  $\mu\text{M}$  ATP and 500 nM ATP reporter-Cy3, 100  $\mu\text{M}$  cocaine, and 500 nM cocaine reporter-Cy3 in 50% serum, row 5), serum sample 6 (250  $\mu\text{M}$  ATP, 500 nM ATP reporter-Cy3, 100 nM human  $\alpha$ -thrombin, and 500 nM thrombin reporter-Cy3 in 50% serum, row 6), serum sample 7 (100  $\mu\text{M}$  cocaine, 500 nM cocaine reporter-Cy3, 100 nM human  $\alpha$ -thrombin, and 500 nM thrombin reporter-Cy3 in 50% serum, row 7), and serum sample 8 (250  $\mu\text{M}$  ATP, 500 nM ATP reporter-Cy3, 100  $\mu\text{M}$  cocaine, 500 nM cocaine reporter-Cy3, 100 nM human  $\alpha$ -thrombin, and 500 nM thrombin reporter-Cy3 in 50% serum, row 8) were created. The mixture was introduced into a tubular DNM sensor and incubated for 30 min at 37  $^\circ\text{C}$ . The washing buffer was then introduced to wash the capillary three times (twice with PBST buffer and once with PBS buffer).

## RESULTS AND DISCUSSION

The DNaPull probes featuring three amino groups and extended aptamer sequences were synthesized by simply mixing four single-stranded DNAs through self-assembly within 2 min.<sup>24</sup> These specifically designed DNA nanostructures were covalently bonded to the surface inside the glass capillary via the amine–aldehyde reaction (Figure 1a). For generating the droplet array inside the glass capillary, different DNaPull probes were immobilized along the glass capillary to form a one-dimensional array without employing a sophisticated and

expensive photolithography procedure.<sup>32</sup> As the sample (e.g., cell or tissue extracts) is applied to the glass capillary, the DNA nanostructure-supported aptamers selectively pull down molecules of interest and their binding partner from the droplet, and then the unbound components are washed away. Captured molecules are then examined using fluorescence microscopy (Figure 1b).<sup>33</sup>

The DNaPull performance in the glass capillary was first evaluated by ATP analysis employing two split fragments of the anti-ATP aptamer.<sup>34</sup> One fragment was appended to the rigid DNA nanostructure inside the glass capillary as the pull-down element. The other was modified with a fluorescein (Cy3) tag to introduce a signal. In the presence of ATP, the two parts of the aptamer were expected to form a sandwich structure; thus, the fluorescein tag was pulled down to the surface and produced a signal (Figure 1c). We challenged the DNaPull assay with a series of concentrations of ATP (from 1  $\mu\text{M}$  to 1 mM). The magnitude of the fluorescent signal increased monotonically with the concentration of ATP (Figure 1d). A control experiment was performed to confirm that the observed fluorescence change was specific to only the binding of ATP with the split aptamer. When three ATP analogues (1 mM each, CTP, GTP, UTP, ADP, and AMP) were employed, the produced fluorescence was merely detectable (Figure 1e). The DNaPull assay exhibited a significantly improved performance ( $\sim 3$ -fold) compared to that of the conventional ssDNA probe-based pull-down assay (Figure 1b,f). We attribute this improvement to the highly rigid and oriented DNA nanostructures in the glass capillary, which accommodates the pendant probe of the DNA tetrahedron with a highly ordered upright orientation to prevent entanglement and local aggregation that are often encountered by soft ssDNA probes.<sup>30</sup>

Rapid sensing capability is a crucial requirement for the successful development of single-step point-of-care diagnostics. Because the transportation of target molecules to the sensing interface is as important in influencing the binding kinetics as the chemical reaction itself,<sup>35</sup> we therefore examined the effect of convection in our DNaPull assay in the glass capillary (Figure 2a). We started with the simplest scenario, in which the target diffuses through the solution and binds immediately upon encountering the sensor surface. Theoretical studies were conducted on the binding reaction process inside the glass capillary under different conditions using a computational fluid dynamic simulation. The target solution flows with a constant



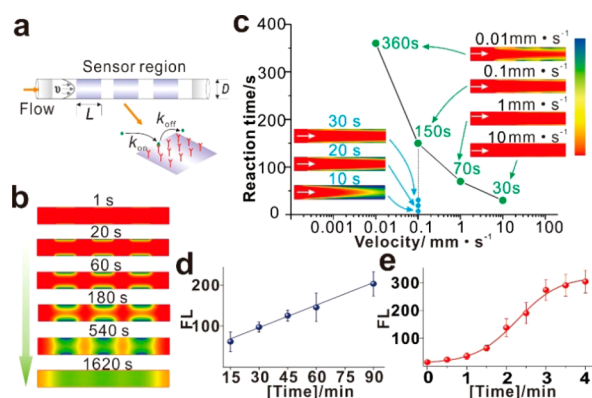


**Figure 2.** Theoretical and experimental studies of the bubble-mediated shuttle reaction process inside the glass capillary. (a) Schematic of the model system. The key simulation parameters were based on our sensing system: glass capillary of inner diameter  $D$  ( $=200\ \mu\text{m}$ ) and a tubular sensing surface of length  $L$  ( $=200\ \mu\text{m}$ ) with a diffusion coefficient of the target solution of  $10\text{--}11\ \text{m}^2/\text{s}$ . (b) Effect of purely diffusive flux (with a flow velocity of  $0\ \text{mm/s}$ ) to the tubular sensing interface (with a  $1\ \mu\text{M}$  target solution). (c) Effect of flow velocity ( $0.01$ ,  $0.1$ ,  $1$ , and  $10\ \text{mm/s}$ ) on the completed reaction time in the glass capillary of the DNaPull assay. The target solution was pressure-driven. Experimental comparison of reaction time between (d) purely diffusive flux and (e) convective flux at a flow rate of  $5\ \mu\text{L}/\text{min}$  (both with  $1\ \text{mM}$  ATP).

velocity ( $v$ ) through a glass capillary with inner diameter  $D$  ( $=200\ \mu\text{m}$ ), and its inner wall contains a sensing surface of length  $L$  ( $=200\ \mu\text{m}$ ) in the flow direction. The sensing surface was functionalized with DNaPull probes, with a surface density of  $10\ \mu\text{M}/\text{m}^2$ . The effect of purely diffusive flux was first evaluated with a setup velocity ( $v$ ) of  $0\ \text{mm/s}$  and a target concentration at  $1\ \mu\text{M}$  under a series of reaction times, including  $1$ ,  $20$ ,  $180$ ,  $540$ , and  $1620\ \text{s}$ . Figure 2b shows the behavior of this ideal DNaPull assay. As targets are pulled down at the sensing interface, a depleted zone is formed ( $20\ \text{s}$ ), which starts relatively flat and then grows radially (between  $20$  and  $540\ \text{s}$ ) until its thickness range is comparable to the length of the sensing surface,  $L$  ( $540\ \text{s}$ ). It then extends into the entire glass capillary ( $1620\ \text{s}$ ). The simulation results suggest that the complete reaction time for all probes at the tubular sensing interface was  $1620\ \text{s}$ . Moreover, our simulation study suggests

that the reaction could be greatly accelerated by adding convective transport, which the target moving along with a fluid flow. For instance, at a target solution concentration of  $1\ \mu\text{M}$ , the reaction was completed within  $30\ \text{s}$  under a flow velocity of  $10\ \text{mm/s}$ , which was shortened approximately 54-fold ( $30\ \text{s}$  vs  $1620\ \text{s}$ ) compared to that of purely diffusive flux (i.e., flow velocity of  $0\ \text{mm/s}$ ). The completed reaction time in the glass capillary of the DNaPull assay decreased monotonically (from  $360$  to  $30\ \text{s}$ ) as the flow velocity increased from  $0.01$  to  $10\ \text{mm/s}$  (Figure 2c), showing that the reaction time is highly dependent on the flow velocity of the target solution. In this scenario, the target would be forced to diffuse into the depleted zone of the sensing interface under a constant continuous flow; therefore, the reaction time was determined by fluid velocity. More importantly, the results of our simulation studies are in agreement with the experimental results observed with the  $1\ \text{mM}$  ATP assay. We found that it took  $>90\ \text{min}$  to complete the ATP pull-down reaction under purely diffusive flux (Figure 2d). By adapting a pressure-driven flow with a volumetric flow rate of  $5\ \mu\text{L}/\text{min}$  inside the DNaPull probe-functionalized glass capillary, we could achieve complete pull down of target molecules within  $4\ \text{min}$  (Figure 2e).

Utilizing a similar theory of ATP sensing, this DNaPull assay in the glass capillary could also be extended to a versatile platform for the quantitative detection of a broad range of biomolecules with high sensitivity. For instance, via incorporation of an anti-cocaine aptamer (Figure 3a),<sup>36,37</sup> a DNaPull assay for cocaine detection was developed. The fluorescence intensities exhibited a nonlinear dependence on the cocaine concentration in the range of  $1\ \mu\text{M}$  to  $1\ \text{mM}$ , with a detection limit of  $1\ \mu\text{M}$  (Figure 3b). Control experiments revealed that analogue molecules of cocaine [benzoylecgonine (BE) and methylecgonine (ME)] produced only very weak responses, demonstrating the high selectivity caused by the intrinsic specificity and affinity properties of DNA aptamers (Figure S3). This DNaPull-based cocaine sensor was further challenged with a variety of cocaine-containing media that were critical to their practical applications (Figure S4). This DNaPull assay showed excellent performance in tainted samples, such as  $10$  or  $50\%$  serum, soda, and sucrose. Furthermore, a similar strategy was used to construct a DNaPull assay for thrombin detection (Figure 3c). We note that the fluorescence signal intensity increased gradually as the thrombin concentration was

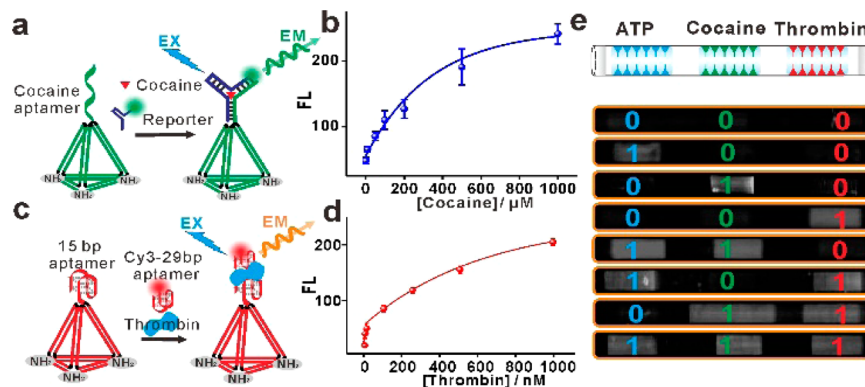


**Figure 3.** (a) Construction of a DNaPull-based cocaine sensor. (b) Fluorescence intensities of DNaPull probes in the presence of  $1$ ,  $10$ ,  $50$ ,  $100$ ,  $200$ ,  $500$ , or  $1000\ \mu\text{M}$  cocaine. (c) Construction of a DNaPull-based thrombin sensor. (d) Fluorescence intensities of DNaPull probes in the presence of  $0.1$ ,  $1$ ,  $10$ ,  $100$ ,  $250$ ,  $500$ , or  $1000\ \text{nM}$  thrombin. (e) Scheme of an array of DNaPull-based sensors inside the glass capillary for the simultaneous detection of ATP, cocaine, and thrombin (top). Fluorescent images of the DNaPull assay recorded from various samples containing different combinations of ATP, cocaine, and thrombin in  $50\%$  serum (bottom).

increased from 0.1 nM to 1  $\mu$ M and showed a limit of detection of 0.1 nM (Figure 3d). It is possible to optimize the performance of the sensor for chemical and biomolecular detection. We investigated the concentration of the Cy3-labeled reporter and noted that the fluorescence signals were dependent on the concentration of the Cy3-labeled reporter, and the optimal concentration was determined to be 500 nM for the detection of thrombin, cocaine, and ATP (Figure S5).

Having evaluated the DNaPull assay performance with a number of representative biomolecules, we further investigated whether such a system could function as a multiplex detection platform in complex matrices. We designed a linear array of the DNaPull assay by immobilizing three types of DNaPull probes (DNaPull-ATP, DNaPull-cocaine, and DNaPull-thrombin) onto the inner wall of the glass capillary in sequential order (Figure 3e) and challenged the system with a series of test samples by dissolving different combinations of ATP, cocaine, and thrombin in 50% serum. The multiplex assay can then be directly read from the microscopic fluorescent images. The addition of a type of biomolecule is defined as the “1” state, and the “0” state corresponds to no addition of biomolecules. Therefore, the output was “000” when neither biomolecule was introduced, corresponding to a blank control (Figure 3e, row 1). The addition of either 250  $\mu$ M ATP (Figure 3e, row 2, “100”), 100  $\mu$ M cocaine (Figure 3e, row 3, “010”), or 100 nM thrombin (Figure 3e, row 4, “001”) caused the fluorescence variations corresponding to the DNaPull probes, which could be defined as the references. On the basis of the results presented above, it is thus possible to use this DNaPull assay to realize multiplex detection. For instance, when both ATP and cocaine were added simultaneously, the output became “110” (Figure 3e, row 5). Similar results can also be obtained when both ATP and thrombin (Figure 3e, row 6, “101”), or both cocaine and thrombin (Figure 3e, row 7, “011”), were introduced into the glass capillary. Finally, the addition of all three types of biomolecules resulted in an increase in the fluorescence intensities in all microarray regions, leading to a “111” state (Figure 3e, row 8). Taken together, these multiplex assay studies clearly indicated that our DNaPull assay could potentially function as a rapid and sensitive point-of-test device for multiplex in vitro bioassays and clinical diagnostics.

It is critically important to evaluate the single-cell analysis applicability of this DNaPull assay by challenging the sensor with cellular ATP from finite cells. We designed a microfluidic device to compartmentalize cells into nanoliter-sized droplets for analysis of all of their ATP. One flow contains a cell suspension with reporters, and the other flow contains a lysis buffer. Once the following droplet formed, the cell was lysed and released its ATP, which was then detected by the DNaPull assay in the glass capillary (Figure 4a). As shown in Figure 4b, a series of different numbers of HNE1 cells (zero to five cells from left to right, respectively) were encapsulated inside a single nanoliter-sized droplet. After lysis, the droplet-containing HNE1 cells produced a fluorescence intensity higher than that of the empty droplet (that contained zero cells), which indicated the successful capture of the released cellular ATP. We noted that the fluorescence intensity increased gradually as the number of cells encapsulated in the droplet was increased from zero to five. In our preliminary experiment, we could quantify the ATP concentration from approximately five cells obtained by encapsulation in nanoliter-sized droplets compared to the  $\sim$ 5000 cells usually required for ATP bioluminescent assay kits.<sup>38</sup> The intracellular ATP level was estimated to be

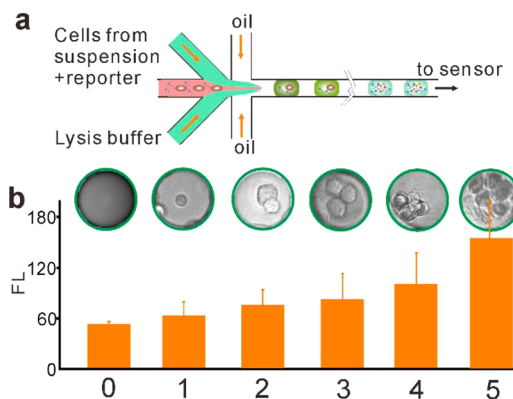


**Figure 4.** (a) Schematic illustrating sample preparation for the cellular ATP assay with nanoliter-sized droplet encapsulation and lysis. (b) Measurement of cellular ATP levels for HNE1 cells (zero to five cells from left to right, respectively) encapsulated inside nanoliter-sized droplets using the DNaPull assay.

$\sim$ 3.4 mM using the DNaPull assay, which was comparable to the result of the analysis ( $\sim$ 2.6 mM) conducted using a commercial ATP bioluminescent somatic cell assay kit.<sup>39</sup> Combining this with single-molecule fluorescence microscopy,<sup>16,40–42</sup> this method can be used to analyze and quantify cellular molecules at a single-cell level.

## CONCLUSION

We developed a rapid DNA nanostructure scaffold-supported aptamer pull-down (DNaPull) assay under convective flux in the glass capillary, the goal being single-cell analysis. This system provides several unprecedented advantages that make it a promising sensor system for the rapid pull-down assay of nanoliter-sized droplets. First, the DNA nanostructure-scaffolded aptamer can greatly improve the biomolecular-recognition capability because of its specific orientation and well-defined spacing for the efficient pull down of various bioactive molecules. Second, the DNaPull reaction could be greatly accelerated by adding convective transport in the glass capillary, because the target is forced to diffuse into the depleted zone of the surface under a constant continuous flow. The convective flux allows complete reaction in  $<$ 5 min (that is an 18-fold improvement compared to the static case, 5 min vs 90 min), thus allowing for a rapid pull-down assay. Third, via construction of a series of biomolecule-responsive DNaPull-based sensors inside the glass capillary, it can serve as a convenient and sensitive platform for analyzing nanoliter- or picoliter-sized droplets, which could present single-cell samples. Lastly, it is envisioned that our method can analyze and quantify cellular molecules at the single-cell level. Given the rapid assay feature and single-cell sample analysis ability, we believe that our analytical platform of convection-driven DNaPull in a glass capillary can provide a new paradigm for biosensor design and significantly advance the field of single-cell analysis.

## ASSOCIATED CONTENT

### Supporting Information

The Supporting Information is available free of charge on the ACS Publications website at DOI: 10.1021/acs.analchem.6b04475.

DNA sequences, immobilization of DNaPull probes in the glass capillary, setup of the laser-induced fluorescence

detection platform, and cell culture and sample preparation for the ATP assay (PDF)

## AUTHOR INFORMATION

### Corresponding Authors

\*E-mail: peihao@chem.ecnu.edu.cn. Telephone: (+86) 021-54345484.

\*E-mail: hongc@xmu.edu.cn.

### ORCID

Yang Tian: 0000-0001-8850-0349

Hao Pei: 0000-0002-6885-6708

### Notes

The authors declare no competing financial interest.

## ACKNOWLEDGMENTS

This work was supported by the Shanghai Pujiang Talent Project (15PJ1401800 and 16PJ1402700), the National Science Foundation of China (Grants 21305151, 21505045, and U1505243), the Natural Science Foundation of Fujian Province of China (2015J01064), and the China Postdoctoral Science Foundation (2015M581565). The authors gratefully acknowledge start-up funding from East China Normal University. L.L. acknowledges the financial support from the “1000 Youth Talents Plan”. The work at Harvard University was supported by the National Science Foundation (DMR-1310266) and by the Harvard Materials Research Science and Engineering Center (DMR-1420570). A.A. extends his sincere appreciation to the Deanship of Scientific Research at King Saud University for funding this work (RG-1436-005).

## REFERENCES

- (1) Huang, B.; Wu, H. K.; Bhaya, D.; Grossman, A.; Granier, S.; Kobilka, B. K.; Zare, R. N. *Science* **2007**, *315*, 81–84.
- (2) Lawson, D. A.; Bhakta, N. R.; Kessenbrock, K.; Prummel, K. D.; Yu, Y.; Takai, K.; Zhou, A.; Eyob, H.; Balakrishnan, S.; Wang, C. Y.; Yaswen, P.; Goga, A.; Werb, Z. *Nature* **2015**, *526*, 131–135.
- (3) Vera-Rodriguez, M.; Chavez, S. L.; Rubio, C.; Pera, R. A. R.; Simon, C. *Nat. Commun.* **2015**, *6*, 7601.
- (4) Tang, F. C.; Lao, K. Q.; Surani, M. A. *Nat. Methods* **2011**, *8*, S6–S11.
- (5) Mazutis, L.; Gilbert, J.; Ung, W. L.; Weitz, D. A.; Griffiths, A. D.; Heyman, J. A. *Nat. Protoc.* **2013**, *8*, 870–891.
- (6) Klein, A. M.; Mazutis, L.; Akartuna, I.; Tallapragada, N.; Veres, A.; Li, V.; Peshkin, L.; Weitz, D. A.; Kirschner, M. W. *Cell* **2015**, *161*, 1187–1201.
- (7) Wang, B. L.; Ghaderi, A.; Zhou, H.; Agresti, J.; Weitz, D. A.; Fink, G. R.; Stephanopoulos, G. *Nat. Biotechnol.* **2014**, *32*, 473–U194.
- (8) Brouzes, E.; Medkova, M.; Savenelli, N.; Marran, D.; Twardowski, M.; Hutchison, J. B.; Rothberg, J. M.; Link, D. R.; Perrimon, N.; Samuels, M. L. *Proc. Natl. Acad. Sci. U. S. A.* **2009**, *106*, 14195–14200.
- (9) Li, L. L.; Wang, W. X.; Ding, M. Y.; Luo, G. A.; Liang, Q. L. *Anal. Chem.* **2016**, *88*, 6734–6742.
- (10) Qu, X. M.; Lin, R. S.; Chen, H. *Progress in Chemistry* **2011**, *23*, 221–230.
- (11) Deshpande, S.; Caspi, Y.; Meijering, A. E. C.; Dekker, C. *Nat. Commun.* **2016**, *7*, 10447.
- (12) Miller, O. J.; El Harrak, A.; Mangeat, T.; Baret, J. C.; Frenz, L.; El Debs, B.; Mayot, E.; Samuels, M. L.; Rooney, E. K.; Dieu, P.; Galvan, M.; Link, D. R.; Griffiths, A. D. *Proc. Natl. Acad. Sci. U. S. A.* **2012**, *109*, 378–383.
- (13) Chang, C.; Sustarich, J.; Bharadwaj, R.; Chandrasekaran, A.; Adams, P. D.; Singh, A. K. *Lab Chip* **2013**, *13*, 1817–1822.
- (14) Chen, F. M.; Lin, L. Y.; Zhang, J.; He, Z. Y.; Uchiyama, K.; Lin, J. M. *Anal. Chem.* **2016**, *88*, 4354–4360.
- (15) Hasic, S. J.; Murthy, S. K.; Koppes, A. N. *Anal. Chem.* **2016**, *88*, 354–380.
- (16) Jain, A.; Liu, R. J.; Ramani, B.; Arauz, E.; Ishitsuka, Y.; Ragunathan, K.; Park, J.; Chen, J.; Xiang, Y. K.; Ha, T. *Nature* **2011**, *473*, 484–488.
- (17) Schmit, V. L.; Martoglio, R.; Carron, K. T. *Anal. Chem.* **2012**, *84*, 4233–4236.
- (18) Nemoto, N.; Fukushima, T.; Kumachi, S.; Suzuki, M.; Nishigaki, K.; Kubo, T. *Anal. Chem.* **2014**, *86*, 8535–8540.
- (19) Pinheiro, A. V.; Han, D. R.; Shih, W. M.; Yan, H. *Nat. Nanotechnol.* **2011**, *6*, 763–772.
- (20) Dietz, H. *Nat. Nanotechnol.* **2015**, *10*, 829–830.
- (21) Wilner, O. I.; Weizmann, Y.; Gill, R.; Lioubashevski, O.; Freeman, R.; Willner, I. *Nat. Nanotechnol.* **2009**, *4*, 249–254.
- (22) Pei, H.; Zuo, X. L.; Pan, D.; Shi, J. Y.; Huang, Q.; Fan, C. H. *NPG Asia Mater.* **2013**, *5*, e51.
- (23) Pei, H.; Liang, L.; Yao, G. B.; Li, J.; Huang, Q.; Fan, C. H. *Angew. Chem., Int. Ed.* **2012**, *51*, 9020–9024.
- (24) Pei, H.; Lu, N.; Wen, Y. L.; Song, S. P.; Liu, Y.; Yan, H.; Fan, C. H. *Adv. Mater.* **2010**, *22*, 4754–4758.
- (25) Tian, Y.; Wang, Y.; Xu, Y.; Liu, Y.; Li, D.; Fan, C. H. *Sci. China: Chem.* **2015**, *58*, 514–518.
- (26) Wen, Y. L.; Pei, H.; Wan, Y.; Su, Y.; Huang, Q.; Song, S. P.; Fan, C. H. *Anal. Chem.* **2011**, *83*, 7418–7423.
- (27) Wang, P. J.; Wan, Y.; Ali, A.; Deng, S. Y.; Su, Y.; Fan, C. H.; Yang, S. L. *Sci. China: Chem.* **2016**, *59*, 237–242.
- (28) Lin, M. H.; Wang, J. J.; Zhou, G. B.; Wang, J. B.; Wu, N.; Lu, J. X.; Gao, J. M.; Chen, X. Q.; Shi, J. Y.; Zuo, X. L.; Fan, C. H. *Angew. Chem., Int. Ed.* **2015**, *54*, 2151–2155.
- (29) Pei, H.; Wan, Y.; Li, J.; Hu, H. Y.; Su, Y.; Huang, Q.; Fan, C. H. *Chem. Commun.* **2011**, *47*, 6254–6256.
- (30) Li, Z. H.; Zhao, B.; Wang, D. F.; Wen, Y. L.; Liu, G.; Dong, H. Q.; Song, S. P.; Fan, C. H. *ACS Appl. Mater. Interfaces* **2014**, *6*, 17944–17953.
- (31) Yang, F.; Zuo, X.; Li, Z.; Deng, W.; Shi, J.; Zhang, G.; Huang, Q.; Song, S.; Fan, C. *Adv. Mater.* **2014**, *26*, 4671–4676.
- (32) Qu, X. M.; Wang, Y. Q.; Shi, Z.; Fu, G. C.; Zeng, X.; Li, X.; Chen, H. *Biosens. Bioelectron.* **2012**, *38*, 342–347.
- (33) Jain, A.; Liu, R. J.; Xiang, Y. K.; Ha, T. *Nat. Protoc.* **2012**, *7*, 445–452.
- (34) Li, F.; Zhang, J.; Cao, X. N.; Wang, L. H.; Li, D.; Song, S. P.; Ye, B. C.; Fan, C. H. *Analyst* **2009**, *134*, 1355–1360.
- (35) Squires, T. M.; Messinger, R. J.; Manalis, S. R. *Nat. Biotechnol.* **2008**, *26*, 417–426.
- (36) Liu, J. W.; Cao, Z. H.; Lu, Y. *Chem. Rev.* **2009**, *109*, 1948–1998.
- (37) Zuo, X. L.; Xiao, Y.; Plaxco, K. W. *J. Am. Chem. Soc.* **2009**, *131*, 6944–6945.
- (38) Szabo, C.; Zingarelli, B.; O'Connor, M.; Salzman, A. L. *Proc. Natl. Acad. Sci. U. S. A.* **1996**, *93*, 1753–1758.
- (39) Zheng, D.; Seferos, S. D.; Giljohann, A. D.; Patel, C. P.; Mirkin, A. C. *Nano Lett.* **2009**, *9*, 3258–3261.
- (40) Peterson, E. M.; Manhart, M. W.; Harris, J. M. *Anal. Chem.* **2016**, *88*, 1345–1354.
- (41) Peterson, E. M.; Manhart, M. W.; Harris, J. M. *Anal. Chem.* **2016**, *88*, 6410–6417.
- (42) Li, W.; Jiang, W.; Dai, S.; Wang, L. *Anal. Chem.* **2016**, *88*, 1578–1584.